Intramolecular Electron Transfer between Doubly Four σ-Bond-Linked Tetraalkylhydrazine Cationic and Neutral Units

Stephen F. Nelsen,* Michael T. Ramm, J. Jens Wolff, and Douglas R. Powell

Contribution from the Department of Chemistry, University of Wisconsin, 1101 University Avenue, Madison, Wisconsin 53706-1396

Received September 30, 1996. Revised Manuscript Received May 4, 1997[⊗]

Abstract: Rate constants k_{ESR} for intramolecular electron transfer between the reduced and oxidized hydrazine units of dimeric 2-*tert*-butyl-3−isopropyl-2,3-diazabicyclo[2.2.2]octylhydrazine radical cations which are doubly linked through the bicyclic units by four σ-bonds (**aBIT**$^+$, **sBIT**$^+$, and **aBIH**$^+$) were determined by simulations of their variable temperature ESR spectra in methylene chloride to be 10.5(7), 9.6(3), and 12.4(4) $\times$ 10^7 s^{-1} at 298 K, respectively. These cations show solvent sensitive charge transfer absorption bands from which the vertical electron transfer excitation energy, λ, and the electronic coupling, V_J, were determined by simulation of the charge transfer bands using vibronic coupling theory (ref 13). Partitioning between solvent and vibrational components of λ was made assuming that the average energy of the vibrational modes coupled to the electron transfer, $h\nu_v$, is 2.29 kcal/mol (800 cm^{-1}). The ESR rate constants at 298 K for **s-** and **aBIT**$^+$ are factors of 23 and 26, respectively, larger than k_{cal}, calculated from λ_s, λ_v, $h\nu_v$, and V_J estimated using a vibronic coupling theory analysis of the charge transfer bands. The ratio $k_{cal}(350)/k_{cal}(250)$ is 7.4 and 9.4($k_{ESR}(350)/k_{ESR}(250)$) for **sBIT**$^+$ and **aBIT**$^+$, respectively. Previously reported data for the doubly-linked four σ-bond dimeric *N,N′*-bis-2,3-diazabicyclo[2.2.2]octyl hydrazine (**22H**$^+$) was also reanalyzed using vibronic coupling theory. k_{ESR}/k_{cal} in acetonitrile at 298 K is 20, but $k_{cal}(350)/k_{cal}(250)$ is 25($k_{ESR}(350)/k_{ESR}(250)$). Possible reasons for the rather poor agreement with theory are suggested.

Introduction

We have been studying organic analogues of mixed-valence complexes,[1] using dinitrogen charge-bearing units which are doubly linked by four-σ-bonds.[2] The tetracyclic and hexacyclic bis-azo compounds **T** and **H** were bis-*tert*-butylated to equal mixtures of diastereomeric bis-diazenium salts. The *tert*-butyl

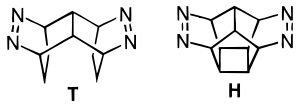

anti and *syn* salts **aBT**$^{2+}$ and **sBT**$^{2+}$ derived from **T** could be separated cleanly by crystallization, but only the *anti* bis-diazenium salt **aBH**$^{2+}$ from **H** was successfully purified and used for these studies. Addition of methyllithium to the bis-

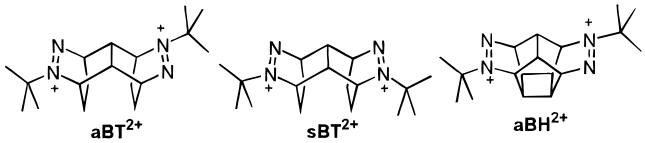

diazenium salts gave bis-hydrazines, shown to exist both in solids and in solution in the "opposite corners *syn*" conformations indicated below.[3]

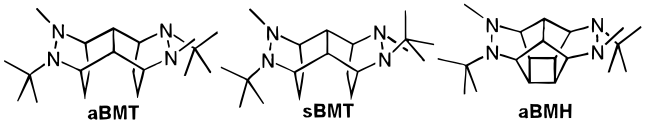

One-electron oxidation of the bis-hydrazines gave radical cations which have charge localized in one hydrazine unit. They exhibit charge transfer (CT) bands in the visible region, which were analyzed using Hush theory.[4] Unfortunately, intramolecular electron transfer (ET) between the hydrazine units is too slow to measure on the ESR time scale,[2] precluding the quantitative comparison of experimentally determined ET rate constants with predictions by theory, which was the goal of this work. These *tert*-butyl,methyl-substituted radical cations also proved to be rather unstable, making high-quality optical measurements difficult. Further restricting the geometry of the hydrazine units by linking the nitrogen substituents in **22H**$^+$ proved to be synthetically rather difficult, but solved the cation instability problem. It also increased the intramolecular ET rate constant

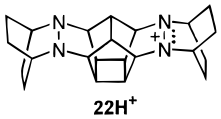

(k_{et}) enough to allow its accurate determination by dynamic ESR as $k_{ESR} = 1.3 \times 10^8$ M^{-1} s^{-1} (at 25 °C in acetonitrile, AN).[5] Although this number appeared satisfyingly consistent with ET

[⊗] Abstract published in *Advance ACS Abstracts*, July 1, 1997.

(1) For a review of transition metal mixed-valence complexes, see: Creutz, C. *Prog. Inorg. Chem.* **1983**, *30*, 1.

(2) (a) Nelsen, S. F.; Chang, H.; Wolff, J. J.; Adamus, J. *J. Am. Chem. Soc.* **1993**, *115*, 12276. (b) There is definite evidence for ion pairing of **22H**$^+$ in chloroform, but not for solvents between AN and MC in polarity, and we assume here that ion pairing effects are negligible for these compounds in this solvent polarity range. (c) An *exo* splitting of ~2.15 was observed for **aBMT**$^+$, but spectral complexity (two different *a*(N) values and a methyl splitting of similar size) and compound instability precluded attempts at the determination of k_{ESR} for the *t*-Bu, Me compounds. See: Chang, H. Ph.D. Thesis, University of Wisconsin, 1992.

(3) Nelsen, S. F.; Wolff, J. J.; Chang, H.; Powell, D, R. *J. Am. Chem. Soc.* **1991**, *113*, 7882.

(4) Hush, N. S. *Coord. Chem. Rev.* **1985**, *64*, 135.

S0002-7863(96)03415-4 CCC: $14.00

Table 1. Structures about the Nitrogens of *t*-Bu,*i*-Pr-Substituted Bis-hydrazines

	aBIH (*i*-Pr both *out*)	**aBIT** (*i*-Pr both *in*)	**sBIT** (*i*-Pr *out*/*i*-Pr *in*)
d(NN) (Å)	1.475(2)/1.475(2)	1.478(4)/1.472(4)	1.482(4)/1.483(4)
α_{av}(N-*t*-Bu) (deg)[a]	112.1(2)/112.3(2)	112.5(3)/112.5(3)	113.5(4)/112.2(4)
α_{av}(N-*i*-Pr) (deg)	112.1(2)/112.1(2)	113.4(3)/112.4(3)	112.5(4)/112.4(4)
θ (deg)[b]	−127.7/−125.9	−129.1/−121.7	131.2/125.2
$\angle C_bNNC_b$ (deg)[c]	3.1(2)/3.3(2)	2.9(4)/7.4(3)	−0.9(4)/−3.0(4)
$\angle C_bCHCHC_b$ (deg)	3.7(2)/4.1(2)	17.1(3)/17.7(3)	−11.5(4)/−11.5(4)
$\angle C_bCH_2CH_2C_b$ (deg)	4.0(2)/4.4(2)[d]	9.3(3)/9.8(3)	−12.1(4)/−11.2(4)
N,N distance (Å)	5.029	4.860	4.861

[a] α_{av} is the average of the bond angles at nitrogen. [b] The lone pair,lone pair dihedral angle, θ, was calculated assuming that the lone pair orbital axes bisect the CNC angle in a Newman projection down the NN bond. [c] C_b is the bridgehead carbon attached to nitrogen. [d] C_bCHCHC_b at the CH carbons of the 4-membered ring.

theory,[6] k_{ESR} for $\mathbf{22H}^+$ is anomalously insensitive to temperature, and unless an apparently unreasonable tunneling efficiency was postulated, the ET parameters derived from the CT band using Hush theory did not fit the observed temperature sensitivity of the k_{ESR} values.[7]

We were very interested to determine if the special structural features imposed by the perbicyclic alkyl substitution of $\mathbf{22H}^+$, which force the hydrazine units to be *cis* (lone pair,lone pair dihedral angles near 0°), as they are in both 0 and +1 oxidation states of the 'monomer' **22/22**, might be responsible for the rather poor agreement with theory. Perhaps the unusual

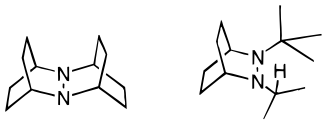

conformational requirements of $\mathbf{22H}^+$ make it an isolated, pathological case. We therefore sought other examples of bis-hydrazine cations for which CT bands could be observed and rate constants measured. Other work demonstrated that having only bicyclic-linked *N*-alkyl groups, as in **22H**, is not necessary for the kinetic protection of hydrazine cations; isopropyl groups suffice, as both the *trans* hydrazine **22/BI** (θ near 120°) and tetraisopropylhydrazine give isolable radical cations.[8] We report here optical and ESR studies of the cations from the doubly linked, four σ-bond dimeric hydrazines **22/BI** (the "monomer"), **aBIT**, **sBIT**, and **aBIH**, which are significantly more stable than their methyl-substituted analogues and have fast enough intramolecular ET to allow k_{ESR} measurement.

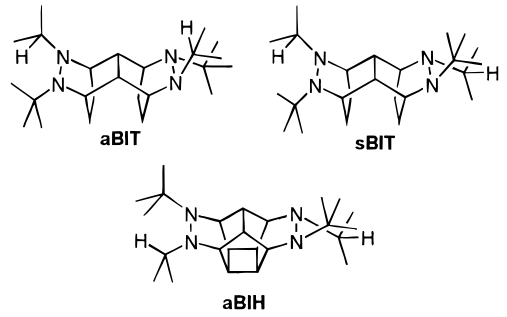

Results

The preparations and solid state structures of **a-** and **sBIT** have been reported,[9] and **aBIH** was prepared by the same method, starting from $\mathbf{aBH}^{2+}$. The structural parameters about the nitrogens for **aBIH** are compared with those for **aBIT** and **sBIT** in Table 1. In contrast to **aBIT**, the isopropyl groups are both directed *out* (away from the central C−C bond of the molecule, as drawn above) in the major conformation of **aBIH** present, although about 8% of the bis-double-nitrogen inversion conformation having both isopropyl groups directed *in* was also detected in the crystal. Only one conformation was detected in solution by ^{13}C NMR (see Experimental Section). It may be noted from the dihedral angles of the two carbon bridges linking the bridgehead carbons α to nitrogen, C_b (designated $\angle C_bCH_nCH_nC_b$ in Table 1), that there is considerably less twist in the hydrocarbon portions of the bicyclooctyl systems for **aBIH** and that the nitrogen lone pair twist angles θ at the two hydrazine units in the crystal differ less than those for either **BIT** diastereomer and lie between the extremes for these compounds. The average distance between the hydrazine units is 0.17 Å (3.5%) larger for **aBIH** than those for the **BIT** compounds, which occurs because linking the alkyl groups in the center of the molecule slightly tilts the hydrazine units away from each other. Comparison of the methylated with the isopropylated tetracyclic-linked system geometries has been done previously,[9] with the conclusion that both larger α_{av} and smaller θ values should make the vertical reorganization energy λ smaller for the isopropylated compounds. From Table 1, $\mathbf{aBIH}^+$ is expected to have a λ similar to that of the $\mathbf{BIT}^+$ compounds.

The thermodynamics for electron loss were studied by cyclic voltammetry (CV). Although both the mono- and dications from these compounds are stable on the CV time scale, broadening from slow electron transfer is obvious at faster scan rates and at platinum, as expected from previous work.[8a] The data reported in Table 2 were taken at a gold electrode using 20 mV/s scan rates, and broadening due to electrochemical quasireversibility apprears to be larger in methylene chloride (MC) than in AN, and for **aBIH** than for the **BIT** diastereomers, which give nearly indistinguishable data. The difference in ease of second and first electron removal (corrected statistically as in our previous work on the methyl-substituted compounds,[2] see Table 2, footnote c) is substantially larger for the isopropylated **BIT** isomers than for their methyl-substituted **BMT** analogues, but nearly the same for the less-twisted **aBIH** and **aBMH**. The difference in ease of first and second electron removal depends upon the electronic interaction between the charge-bearing units as well as the work term for forming one cation near another and any solvation or ion-pairing[2b] energy

(5) Nelsen, S. F.; Adamus, J.; Wolff, J. J. *J. Am. Chem. Soc.* **1994**, *116*, 1589.

(6) For ET theory reviews, see: (a) Sutin, N. *Prog. Inorg. Chem.* **1983**, *30*, 441. (b) Marcus, R. A.; Sutin, N. *Biochim. Biophys. Acta* **1985**, *811*, 265.

(7) Nelsen, S. F. *J. Am. Chem. Soc.* **1996**, *118*, 2047.

(8) (a) Nelsen, S. F.; Chen, L.-J.; Petillo, P. A.; Evans, D. H.; Neugebauer, F. A. *J. Am. Chem. Soc.* **1993**, *115*, 10611. (b) Nelsen, S. F.; Chen, L.-J.; Powell, D. R.; Neugebauer, F. A. *J. Am. Chem. Soc.* **1995**, *117*, 11434.

(9) Nelsen, S. F.; Ramm, M. T.; Wolff, J. J.; Powell, D. R. *J. Org. Chem.* **1996**, *61*, 6313.

Table 2. Cyclic Voltammetry Data

cmpd	solvent[a]	$E_1^{\circ\prime}(\Delta E_{pp})$ (V (mV)[b]	$E_2^{\circ\prime}(\Delta E_{pp})$ (V (mV)[b]	$\Delta E^{\circ\prime}$ (kcal/mol)[c]	Δ(Me → *i*-Pr) (kcal/mol)
aBIT	AN	−0.20(64)	+0.04(68)	4.7	2.3
	MC	−0.09(114)	+0.16(108)	4.9	2.1
	DMF	−0.08(94)	+0.12(84)	3.6	
sBIT	AN	−0.21(70)	+0.03(72)	4.7	2.0
	MC	−0.10(118)	+0.15(108)	4.9	2.3
aBIH	AN	−0.05(99)	+0.18(99)	4.3	0.05
	MC	+0.07(124)	+0.26(102)	3.7	−0.1

[a] AN = acetonitrile, MC = methylene chloride, DMF = *N*,*N*-dimethylformamide. [b] $E_1^\circ = (E_p^{ox} + E_p^{red})/2$, given in V vs SCE; $\Delta E_{pp} = (E_p^{ox} - E_p^{red})$, given in mV. [c] $\Delta E^{\circ\prime}$ (kcal/mol) = $23.06(E_2^\circ - E_1^\circ - 0.036)$. [d] Increase in ΔE° upon replacing methyl by isopropyl.

differences caused by changing substitutents. Some have tried to extract the ET parameter *V* (see below) from differences in $\Delta E^{\circ\prime}$, but it appears clear to us that the differences in $\Delta E^{\circ\prime}$ between **BIT** and **BMT** must be principally caused by differences in solvation energies, because the linking frameworks between the charge-bearing units are identical in these systems; thus, differences in both the work term and *V* are expected to be very small.

The principal reason for studying these isopropyl-substituted compounds was to increase cation stability so that reliable optical and ESR data could be obtained. Coulometric oxidation in a modified cyclic voltammetry cell in which a platinum mesh working electrode was separated from a silver wire counter-electrode by a fine porous glass frit was performed at 0.3 V positive of $E_1^{\circ\prime}$, in solutions containing 0.1 M tetrabutylammonium perchlorate. Chemical oxidations used silver nitrate in acetonitrile, ($E_p^{red} \approx 0.35$ vs SCE), followed by filtration through Celite to remove silver metal. These methods gave λ_{max} and ϵ_{max} values within experimental error of each other, despite the presence of supporting electrolyte in the electrochemical oxidation. In addition to the CT band in the visible, a more intense, sharper band at 290 nm corresponding to π,π^* excitation of the hydrazine cation unit appears. This band is also present in the optical spectrum of **22/BI**$^+$, the "monomer" for these systems. In contrast to **22H**$^+$, the isopropyl-substituted cations are not completely stable in solution. As they decompose, large changes take place below 300 nm in the UV spectrum, and the visible maximum decreases in intensity and shifts to slightly longer wavelength; however, less than 10% loss of absorption at the CT band maximum occurs over a period of 10 h at room temperature and negligible loss occurs during the approximately 25 min it takes to prepare a sample and obtain optical data. It was demonstrated that neither band shape nor ϵ_{max} changes upon 5-fold dilution of a sample, so any possible intermolecular effects are not detectable. The optical spectral

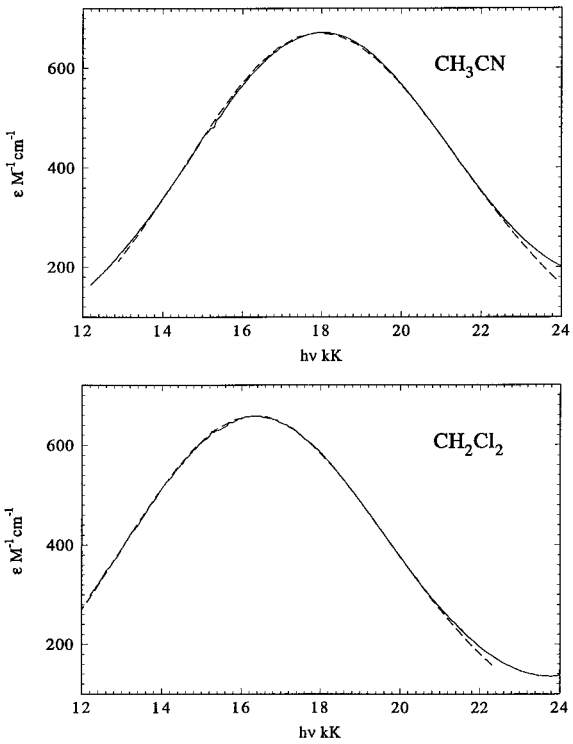

Figure 1. CT band absorption for **aBIT**$^+$ in acetonitrile and methylene chloride. The dotted lines superimposed on the experimental data show fits calculated using eq 3 with the following parameters: CH_3CN λ = 54.00 kcal/mol, V_J = 3.30 kcal/mol, $h\nu_{in}$ = 800 cm^{-1}, λ_s = 22.95 kcal/mol; CH_2Cl_2 λ = 49.47 kcal/mol, V_J = 2.99 kcal/mol, $h\nu_{in}$ = 800 cm^{-1}, λ_s = 18.52 kcal/mol.

data for the CT bands are summarized in Table 3, and the absorption curves for **aBIT**$^+$ in two solvents appear in Figure 1. The doubly oxidized bis-cations show a visible band with approximately four times the ϵ_{max} value of the monocations, which occurs near the minimum absorption region for the monocations and has less solvent sensitivity than the CT band of the monocations. For **aBIT**$^{2+}$ λ_{max}(AN) = 420 nm (ϵ_{max} = 2560 M^{-1} cm^{-1}), λ_{max}(MC) = 430 nm (ϵ_{max} = 2340 M^{-1} cm^{-1}). Their very different absorption spectra make it clear that our samples of monocation are not significantly contaminated with bis-cation. Although the bis-cations are very stable in solution and appear to be isolable as solids, their crystals proved to be twinned, and we were unable to obtain X-ray crystallographic structures.

A further demonstration that the long wavelength absorption band of the monocations is a charge transfer band was provided by addition of an equivalent of $HBF_4 \cdot Et_2O$. The CT band instantly disappears, as expected when the neutral hydrazine

Table 3. CT Band Visible Spectral Data for Bis-hydrazine Radical Cations

compd	**aBIT**$^+$				**sBIT**$^+$				**aBIH**$^+$		
solvent[a]	AN	BN	DMF	MC	AN	BN	DMF	MC	DCE	AN	MC[b]
λ_{max} (nm)	554	560	546	610	556	560	538	610	610	588	658
E_{op} (10^{3}cm^{-1})	18.1	17.9	18.3	16.4	18.0	17.9	18.6	16.4	16.4	17.0	15.2
E_{op} (kcal/mol)	51.6	51.1	52.4	46.9	51.4	51.1	53.2	46.9	46.7	48.6	43.5
ϵ_{max} (M^{-1} cm^{-1})	672	664	419	659	666	648	588	647	688	424	413
$\Delta\nu_{1/2}$ (10^{3}cm^{-1})	8.31	8.13	7.84	7.94	8.26	8.08	9.11	8.04	7.83	8.31	9.93
Hush V_H° (kcal/mol)	3.8	3.8	3.0	3.6	3.8	3.7	3.8	3.6	3.6	2.9	3.0
λ (kcal/mol)[a]	54.0	53.5	54.9	49.5	54.1	53.4	56.2	49.7	49.3	51.7	47.5
V_J (kcal/mol)	3.3	3.2	2.5	3.0	3.3	3.2	3.2	3.0	3.0	2.5	2.3
λ_s(800) (kcal/mol)[c]	23.0	24.0	31.6	18.5	22.0	24.5	15.2	17.5	21.1	16.4	6.3
λ_v(800) (kcal/mol)[c]	31.1	29.5	23.3	30.8	32.1	28.9	41.0	32.3	28.2	35.3	41.2
k_{calcd} (10^{5}s^{-1})	7.3			41	7.7			42			[190]

[a] Solvent abbreviations as in Table 2 plus BN = butyronitrile, DCE = 1,2-dichloroethane. [b] This data set appears to be flawed; see text. [c] λ_s, λ_v partitioning assuming $h\nu_v$ = 2.29 kcal/mol (800 cm^{-1}). [d] Calculated at 298 K using the ET parameters given with eq 10.

Table 4. Dynamic ESR Rate Constants and Activation Parameters for ET within Four σ-Bond-Linked Bis-hydrazine Radical Cations

cmpd	solvent	T range (K)	k_{298} (10^7 s^{-1})	$\Delta G^{\ddagger}(298)$ (kcal/mol)[a]	$\Delta H^{\ddagger}$ (kcal/mol)[a]	$\Delta S^{\ddagger}$ (cal mol^{-1} K^{-1})[b,c]	k_{ESR}/k_{cal} (298 K)
22H^{+} [b]	AN	250−350(100)	13.2(4)	6.38(2)	0.66(13)	−19.2(4)	20
aBIT^{+}	AN	[single T]	2.6				36
sBIT^{+}	AN	[single T]	2.6				34
aBIT^{+}	MC	264−304(40)	10.5(7)	6.51(4)	3.0(6)	−11.8(21)	26
sBIT^{+}	MC	264−304(40)	9.6(3)	6.57(3)	3.3(3)	−10.9(10)	23
aBIH^{+}	MC	283−308(25)	12.4(4)	6.41(2)	4.0(7)	−8.2(22)	[6.6][c]

[a] Numbers in parentheses are statistical error (only!) in the last digit quoted, at the 95% confidence level. [b] Data from ref 5. [c] The optical data set used for this rate constant is internally inconsistent (see text).

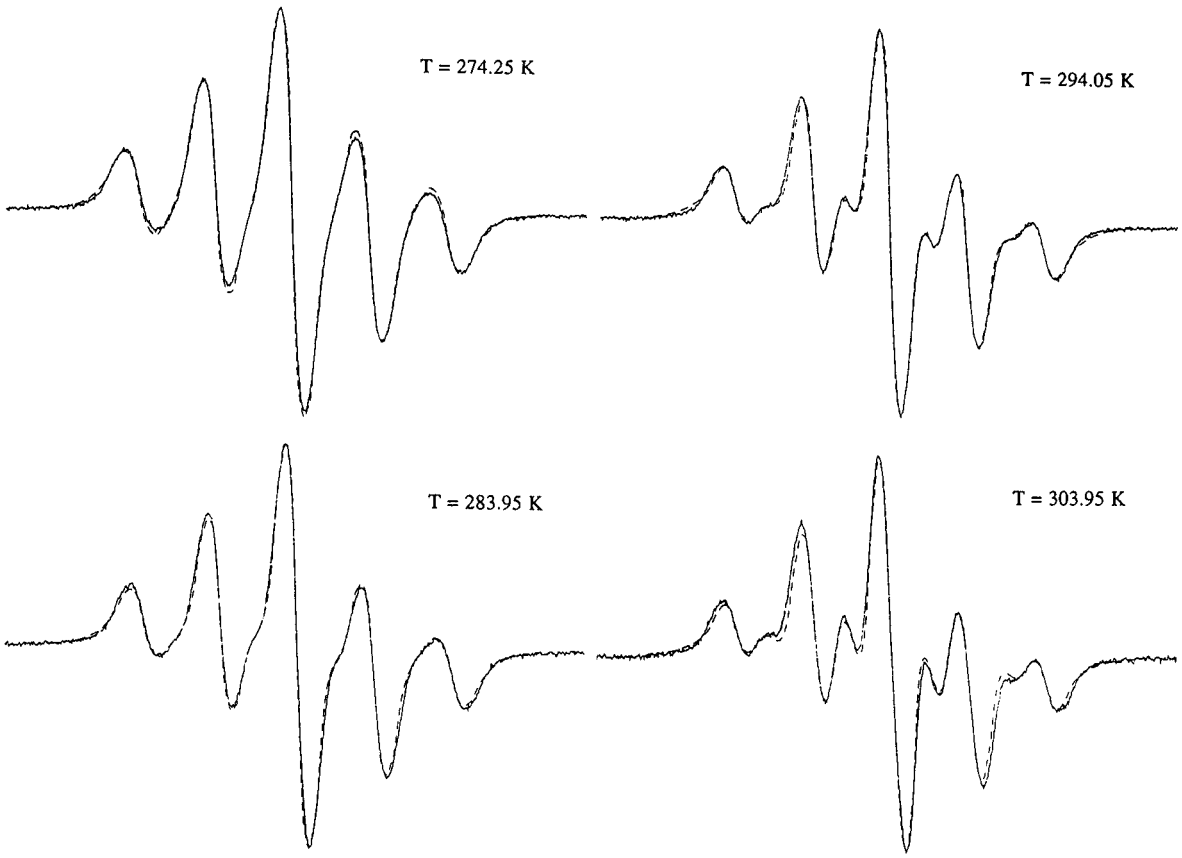

Figure 2. ESR spectra of **sBIT**$^{+}$ in methylene chloride, overlaid with the results of simulations (dotted lines) employing a(2N) = 13.3 G, a(2H) = 2.6 G, and a(4H) = 0.6 G, with line width = 1.1 G and the following k_{ESR} values: 274 K, 5.3×10^7 s^{-1}; 284 K, 7.0×10^7 s^{-1}; 294 K, 9.1×10^7 s^{-1}; 304 K, 10.5×10^7 s^{-1}.

unit becomes protonated and can no longer donate an electron. The bis-cation spectrum is produced within minutes after adding acid in MC, but the conversion takes days in AN. This shows that the equilibrium **2BIT**$^{+}$**-H**$^{+}$ ⇌ **BIT**$^{2+}$ + **BIT-H$_2$**$^{2+}$ lies significantly to the right, but we do not know why the difference in rate of the equilibration is so large. Solutions of **BIH**$^{2+}$ and both diastereomers of **BIT**$^{2+}$ exhibit the expected five-line ESR spectra, but they do not show ESR signals in glasses at liquid nitrogen temperature, suggesting that the triplet relative spin orientations of these bis-radical-cations may be too much higher in energy than the singlet one.

The ESR spectrum of the "monomer" radical cation **22/BI**$^{+}$ only has the five-line pattern for the two approximately equal nitrogen splittings, a(2N) = 13.2 G, resolved. All of the proton splittings except that of the bridgeheads, which must be very small, were determined using a combination of ENDOR and NMR measurements: a(2H) = 2.61, a(2H) = 2.50, a(2H) = −0.63, a(2H) = −0.57, a(1H, *i*-PrCH) = 1.4, a(6H, *i*-PrMe) = 0.27, a(9H, *t*-Bu) = −0.08 G.[8a] The *t*-Bu signal might conceal the bridgehead signals. The larger proton splittings are caused by the methylene hydrogens *exo* to the nitrogens. The ESR spectra of all three "dimeric" radical cations at room temperature in acetonitrile show a two nitrogen quintet splitting indistinguishable from that of **22/BI**$^{+}$, demonstrating that ET is slow on the ESR time scale for the nitrogen splitting constant. However, in the presence of acid, which precludes ET by protonating the unoxidized hydrazine unit, the ESR spectra of both **BIT**$^{+}$ diastereomers exhibit an a(2H) ≈ 2.6 G splitting, as expected when the spin is localized on one hydrazine unit, because two *exo* hydrogens are present. Such a splitting is not present in the spectrum of acidified **aBIH**$^{+}$, which has all four *exo* hydrogens replaced by alkyl substituents. Fast enough ET is occuring for **aBIT**$^{+}$ and **sBIT**$^{+}$ to cause broadening of the 2.6 G splitting, but k_{et} is not fast enough to show detectable effect on the larger, a(N) intensities. Simulation of the spectra for unprotonated **aBIT**$^{+}$ and **sBIT**$^{+}$ using a(2N) = 13.3, a(2H) = 2.6, a(4H) = 1.6, and a 1.5 G line width gave the best fit for $k_{ESR}(298) = 2.6 \times 10^7$ s^{-1}. The *i*-Pr-substituted cations appear to show faster ET than their methylated analogues.[2c] ET reactions are significantly faster in MC than in AN because of a smaller solvent reorganization term (λ_s) in the less-polar solvent, and all three compounds show alternating line width effects in their a(N) features near room temperature. Simulations of the ESR spectra as a function of temperature gave the

data shown in Table 4, and sample simulated spectra are shown in Figure 2.[10] Unfortunately, decomposition became too fast above 310 K for spectra to be accurately determined, limiting the temperature range available for these k_{ESR} measurements. The interpolated k_{ESR}(298 K) values in MC for the *trans* hydrazine unit *i*-Pr,*t*-Bu-substituted compounds are only slightly smaller than that in AN for the *cis* hydrazine unit perbicyclic-substituted **22H**$^+$.

Discussion. 1. Background for Hush and Jortner Theory Analysis of ET Parameters

The Hush theory analysis[4] of the optical data used in our previous work on organic analogues of intervalence complexes[2,3,5] assumes that the transition energy at the CT band maximum, E_{op}, is equal to the Marcus vertical transition energy, $\lambda = \lambda_s + \lambda_v$. We used Hush's eq 1 (eq 25 in ref 4) to evaluate the "off-diagonal matrix term" V, which is equal to half of the energy separation of the ground and excited state adiabatic energy surfaces at the avoided crossing, from the maximum extinction coefficient ϵ_{max} (M^{-1} cm^{-1}), the CT band width at half-height, $\Delta\nu_{1/2}$ (cm^{-1}), E_{op}(cm^{-1}), and the electron transfer distance, d (Å). However, when a more modern vibronic

$$V_H(cm^{-1}) = (2.06 \times 10^{-2})(\epsilon\Delta\nu_{1/2}E_{op})^{1/2}/d \qquad (1)$$

coupling analysis, which we will call Jortner theory,[11] is employed, there is no longer any special significance for E_{op}. Jortner theory uses Franck Condon (FC(g)) factors to calculate the probability of transitions between the initial and final states for the ET (see eq 2A−C for the formulation appropriate for the analysis of CT bands), which makes the vibronic coupling factor S of fundamental importance in determining V. Jortner

$$FC(g) = \Sigma_w F_w(4\pi\lambda_s k_B T)^{-1/2} \times \exp(-[wh\nu_v + g + \lambda_s]^2/4\lambda_s k_B T) \qquad (2A)$$

$$S = \lambda_v/h\nu_v \qquad (2B)$$

$$F_w = e^{-S}S^w/w! \qquad (2C)$$

has discussed the application of eq 2 to fluorescence emission bands,[12] but the Kodak group has considered its application for CT absorption bands as well.[13] They obtain eq 3 (eq 4 in ref 13), where N is Avagodro's number, c the speed of light, n is the refractive index of the solvent, $\Delta\mu$ the change in dipole moment upon absorption of light, which using the same assumptions as Hush may be replaced by $e\cdot d$, ν is the frequency (s^{-1}), and the appropriate g value for a CT absorption band of a symmetrical CT intervalence complex has been employed.

$$\epsilon\nu = [(8N\pi^3)/3000h^2c\ln(10)]\, nV^2\Delta\mu^2 FC(-h\nu) \qquad (3)$$

Using the single $h\nu_v$ version of Jortner theory adopted for this work, the reaction coordinate accounts for only the solvent portion of the vertical excitation energy, and the energy surfaces consist of stacked initial and final state parabolas separated by $h\nu_v$, having a vertical energy separation between the $\upsilon = 0$ initial minimum and the vertical $w = 0$ final state of λ_s (see Figure 3). The absorption spectrum in an ϵ vs $h\nu$ plot consists a series of overlapping, almost Gaussian subspectra (they are exactly Gaussian if $\epsilon\nu$ is plotted vs $h\nu$)[13] with intensities calculated by eq 2. The highest intensity subspectrum is that for the $0 \rightarrow w$ transition with w closest to S, and intensity becomes increasingly small as w becomes further from S. In applying eq 1 to fluorescence spectra, Jortner and co-workers comment that the relation (changed to our nomenclature) $\lambda + \Delta G \approx E_{op}$ remains fulfilled, as required, and later point out that the approximation errs for the fluorescence spectra discussed by about 1 kcal/mol.[12] For the $\Delta G = 0$ case of a symmetrical intervalence complex, eq 3 does not give maxima in either ϵ or FC(g) at $h\nu = \lambda$. The transition energy at the maximum of the ϵ vs $h\nu$ curve (E_{op}) is smaller than λ by an amount which depends upon all four of the fundamental ET parameters (λ_s, λ_v, $h\nu_v$, and V) and is in the range 2.7 ± 0.4 kcal/mol for the four σ-bond-linked compounds we consider here.

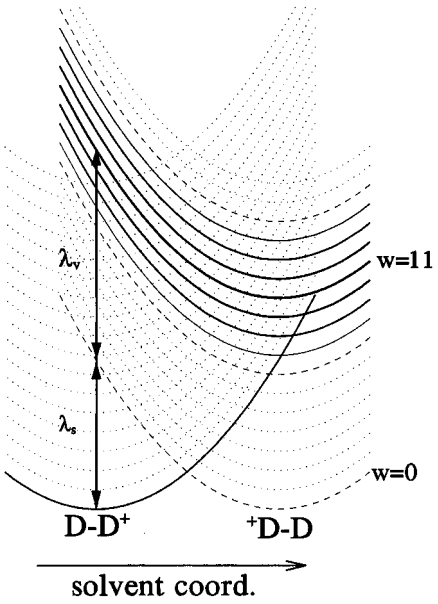

Figure 3. Jortner theory energy diagram for a hypothetical case having $h\nu_v$ = 800 cm^{-1}, λ_s = 17.7 kcal/mol, and λ_v = 25.3 kcal/mol. The most intense CT band subspectrum corresponds to the transition from $\upsilon = 0$ of the ground state well to the $w \approx S = 11$ product state parabola and is centered at $\lambda + 11h\nu_v$. Intensity drops off rapidly as w becomes increasingly far from S, as indicated qualitatively by decreasing width for the product well parabola lines.

Solving for V and inserting the units used above for eqs 1 and 2 gives eq 4 for calculation of V at $h\nu_{max}$ using vibronic coupling theory. Equations 1 and 4 are obviously related and,

$$V_J(cm^{-1}) = (1.995 \times 10^{-2})(\epsilon h\nu_{max}FC(-h\nu_{max})^{-1})^{1/2}/(dn^{1/2}) \qquad (4)$$

despite their different appearance, are within a few percent of differing just by the factor of $n^{1/2}$ which appears only in the V_J expression: $V_H \approx n^{1/2}V_J$.[14]

Discussion. 2. ET Parameters from CT Band Fits for 22H$^+$

A comparison of analyses of the optical data for **22H**$^+$ at 25 °C in AN using Hush[5] and Jortner theory appears as Table 5. Although Hush's theory was derived assuming $h\nu_v < k_BT$, it

(10) For figures showing the complete UV−vis spectra of the three **BI**$^+$ compounds studied, more fits to eq 4, and all of the ESR simulations overlaid upon the experimental ESR spectra, see: Ramm, M. T. Ph.D. Thesis, University of Wisconsin, 1996.

(11) (a) Ulstrup, J.; Jortner, J. *J. Chem. Phys.* **1975**, *63*, 4358. (b) Jortner, J.; Bixon, M. *J. Chem. Phys.* **1988**, *88*, 167.

(12) Cortes, J.; Heitele, H.; Jortner, J. *J. Phys. Chem.* **1994**, *98*, 2527.

(13) Gould, I. R.; Noukakis, D.; Gomez-Jahn, L.; Young, R. H.; Goodman, J. L.; Farid, S. *Chem. Phys.* **1993**, *176*, 439.

(14) A referee pointed out that the close agreement of V_H and $n^{1/2}V_J$ is probably fortuitious because Hush notes that although the theoretical value to use in the denominator of eq 1 is αd, where $\alpha = 0.5$, "we shall assume in what follows that $\alpha = 1$" (p 146).[4] We have not seen an application of eq 1 to experimental data using any value other than $\alpha = 1$.

Table 5. Comparison of Hush and Jortner Analyses of Optical Data for **22H**$^+$ in AN at 298 K[a]

	Hush analysis		Jortner analysis		
λ (kcal/mol)	46.5$_7$		49.4$_5$ ($\lambda - E_{op} = 2.9$)		
V (kcal/mol)	3.76(V_H)		3.22 (V_J)		
$h\nu_v$ cm^{-1} (kcal/mol)	V_H[b]	$\Delta\nu_{1/2}$ (m^{-1})[c]	V_J[b]	λ_s[b]	k_{et} (10^6 s^{-1})
900(2.57)	3.97	0.913	3.224	23.2	5.0
850(2.43)	3.92	0.891	3.223	20.3	5.4
800(2.29)	3.87	0.868	3.223	16.7	5.8
750(2.14)	3.82	0.845	3.223	11.8	6.6
730(2.09)			3.223	9.5	6.9
700(2.00)	3.77	0.823			

[a] Using $d = 5.03$ Å (X-ray value for **aBIH**), thus the entries differ slightly from those of ref 5. [b] Unit, kcal/mol. [c] Predicted using Hush's formula for calculating V using a theoretical line width (eq 28[4]), V_H (cm^{-1}) $= 0.143\epsilon^{1/2}E_{op}3/4U^{1/4}$ coth$(U)^{1/2}/d$, where $U = h\nu_v/2k_BT$. The observed $\Delta\nu_{1/2}$ is 0.821 m^{-1}, so a Hush analysis using the theoretical line width gives $h\nu_v$ near 700 cm^{-1}.

has often been applied to higher $h\nu_v$ cases.[4] Unambiguous extraction of the four ET parameters from Jortner fits to fluorescence CT bands has sometimes been a problem because of the interaction between the parameters which allow multiple value fits.[12,15] For the present cases, fit to the absorption CT band only determines λ and V_J if all four ET parameters are considered to be variables. The λ_s,λ_v partitioning is quite sensitive to $h\nu_v$, but indistinguishable ϵ; $h\nu$ plots having the same values of λ and V_J are obtained using $h\nu_v$ values ranging from 950 to 730 cm^{-1}, although λ_s must be lowered from 52 to 19% of λ to maintain the fit. We note that in contrast to Hush theory, the band width in Jortner theory is not determined simply by $h\nu_v$, but by the combination of $h\nu_v$ and λ_s. Because a dielectric continuum model is consistent with λ_s(AN) $\cong$ 10 kcal/mol for **22H**$^+$ (see below), Jortner theory is consistent with the low $h\nu_v$ value obtained from dynamics calculations which gave $h\nu_v \approx 827$ cm^{-1},[7] and a somewhat smaller value is consistent with the $\Delta\nu_{1/2}$ prediction by Hush theory (Table 5, footnote *b*). The Hush V_H is 0.8% larger than $n^{1/2}V_J$.

The λ for intervalence compounds has traditionally been separated into λ_v and λ_s using the solvent effect on the CT band maximum, employing the Hush and Marcus assumption that $E_{op} = \lambda$ and the Marcus dielectric continuum formula 5, which employs bulk solvent parameters, the refractive index n and the static dielectric constant ϵ_s to estimate the solvent polarity parameter γ. Figure 4 and Table 6 compare the use of Jortner and Hush theory to analyze the solvent effect on the CT band of **22H**$^+$. According to eq 5, λ_v is the intercept of λ vs γ or E_{op} vs γ plots, so λ_s for various solvents can be obtained by subtraction. Because the λ value obtained using Jortner theory

$$\lambda_s(\text{kcal/mol}) = 332.1(r^{-1} - d^{-1})\gamma \qquad (5A)$$

$$\gamma = (n^2)^{-1} - \epsilon_s^{-1} \qquad (5B)$$

is higher than E_{op}, the λ_v and λ_s values obtained are higher. Considering only MC and AN, eq 6 may be written from their γ values (Table 6). Equation 6 produces λ_s(AN) = 9.5 kcal/

$$\lambda_s(CH_3CN) = 3.641\,[E_{op}(CH_3CN) - E_{op}(CH_2Cl_2)] \qquad (6)$$

mol using the $\lambda = E_{op}$ assumption, and λ_s(AN) = 9.8 kcal/mol using the λ values obtained from fitting the CT bands using Jortner theory. Also using data from the four other solvents of intermediate polarity (shown graphically in Figure 4) gives λ_v = 37.6 and λ_s(AN) = 9.0 using the Hush $E_{op} = \lambda$ assumption and 39.15 and 10.3 kcal/mol, respectively, using the λ values obtained from the Jortner theory fits to the bands. Dimethyl sulfoxide gives significantly larger deviations in the plots in Figure 4 than the other solvents, lying 1.3$_7$ kcal/mol above the regression line in the λ plot, and 0.5$_3$ kcal/mol in the E_{op} plot. The chloroform data were not used in the regressions because this significantly less-polar solvent clearly produces higher E_{op} and λ than predicted, which we have attributed to the onset of significant ion pairing.[2a]

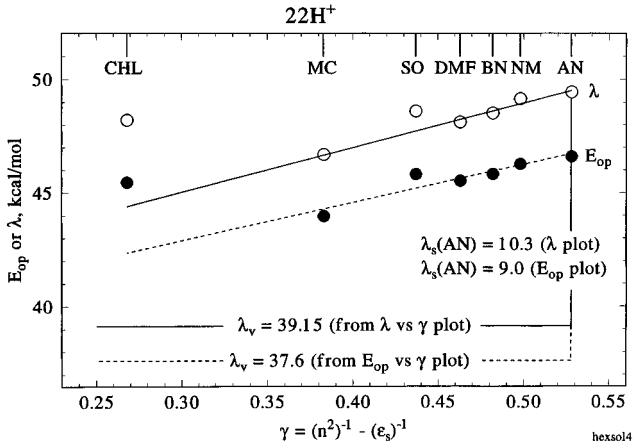

Figure 4. Comparison of Hush theory E_{op} vs γ and Jortner theory λ vs γ plots for **22H**$^+$ (data of Table 6).

Table 6. Solvent Effect on **22H**$^+$ CT Band Parameters: Jortner Analysis

solvent[a]	AN	NM	BN[b]	DMF	SO[c]	MC	CHL
γ	0.528	0.498	0.482	0.463	0.437	0.383	0.268
E_{op} (kcal/mol)	46.6	46.3	45.8	45.5	45.8	44.0	45.5
ϵ (M^{-1} cm^{-1})	771	840	800	850	889	698	807
λ (kcal/mol)	49.4	49.1	48.5	48.1	48.6	46.7	48.2
V_J (kcal/mol)	3.22	3.27	3.20	3.16	3.24	3.23	3.13
$\lambda_s(750)$[d]	11.8	15.7	9.2	17.9	10.9	11.5	
$\lambda_v(750)$[d]	37.6	33.4	39.3	30.2	37.7	35.2	

[a] Solvent abbreviations as in Tables 2 and 3 plus NM = CH_3NO_2, SO = dimethyl sulfoxide, CHL = chloroform. [b] Six percent dication subtracted before analysis. [c] Three percent dication substracted before analysis. [d] Evaluated for $h\nu_v = 2.14$ kcal/mol (750 cm^{-1}); k_{cal}(298 K, AN) using these parameters in eq 10 is 6.55×10^6 s^{-1}.

Equation 5a contains the distance factor in its most simple form, $(r^{-1} - d^{-1})$, where r is the radius of the charge-bearing unit and d the electron transfer distance. This distance factor appears consistent with experiment for **22H**$^+$, because using $d = 5.03$ Å (the X-ray distance between the hydrazine units of **aBIH**, which has the same framework linking the hydrazine units as **22H**) with λ_s(AN) in the range of 9−10.3 kcal/mol produces an effective r value of 3.94 ± 0.06 Å, which is consistent with the average radius for the "monomer" hydrazine, **22/22**, in its crystal, which is 3.95 Å.[15]

Both $V_J = 3.22 \pm 0.06$ kcal/mol and $(\lambda - E_{op}) = 2.75 \pm 0.16$ kcal/mol are satisfyingly constant for all seven solvents studied. The λ_s and λ_v values obtained from Jortner theory CT band fits in each solvent give considerable scatter from the expectation that λ_s will be proportional to γ and λ_v constant. The λ_v values evaluated at $h\nu_{in} = 750$ cm^{-1} average to 35.6 kcal/mol (range +3.7(12%) to −5.3[15%] deviation); lowering $h\nu_v$ lowers λ_s, thus raising λ_v (see Table 5 for this effect in acetonitrile). The only pattern we can distinguish for the λ_s values shown in Table 6 is that the lowest ones were found for butyronitrile and dimethyl sulfoxide, for which the samples were slightly contaminated with dication, and 6% and 3% of the dication spectrum was subtracted from before analysis. Perhaps

(15) Nelsen, S. F.; Blackstock, S. C.; Haller, K. J. *Tetrahedron* **1986**, *42*, 6101.

the subtraction was not sucessful enough, and these solvents should be excluded for this purpose? Excluding them lowers the average λ_v to 34.1 kcal/mol (+3.5, −3.9), not improving the constancy of λ_v much. We conclude that small changes in CT band shape significantly affect the λ_s,λ_v partitioning obtained and that extracting this partitioning from an eq 4 fit to our absoption curves is unlikely to be very accurate. The observed CT bands are so close to being two half-Gaussian curves with only a small difference in the high $h\nu$ and low $h\nu$ band half widths that expecting to extract reliable values for all four ET parameters from them seems to us to be unreasonably optimistic.

In summary, using the Hush and Marcus assumption that $E_{op} = \lambda$ for **22H**$^+$ in AN lowers λ (by 2.85 kcal/mol, 6%), λ_v (by 1.55 kcal/mol, 4%), and λ_s (by 1.3 kcal/mol, 13%) relative to evaluating λ using Jortner theory, and using Hush's eq 1 instead of eq 3 raises the *V* estimate by 0.54 kcal/mol (17%).

Discussion. 3. ET Parameters from CT Band Fits for the *t*-Bu,*i*-Pr-Substituted Compounds

Table 3 contains analysis of the CT bands observed for the *trans*-bis-hydrazine radical cations **aBIT**$^+$, **sBIT**$^+$, and **aBIH**$^+$. The CT bands may be fit rather well using eq 4 (see Figure 1 for sample fits). The two diastereomers of **BIT**$^+$ are expected to behave nearly the same, and having data sets for both of them is probably more useful in indicating the size of experimental errors than anything else. The E_{op} values for **aBIT**$^+$, **sBIT**$^+$, and **aBIH**$^+$ are about 3.9, 4.4, and 3.6 kcal/mol, respectively, smaller than those less accurately determined for their methylated analogues, as expected because flattening at nitrogen and decreasing NN bond twist will lower λ_v. The λ-(AN) values for the more twisted **BIT**$^+$ diastereomers are 2.3−2.4 kcal/mol higher than for **aBIH**$^+$ and 4.6−4.7 kcal/mol higher than for **22H**$^+$.

The V_J values obtained for **aBIT**$^+$ and **sBIT**$^+$ are the same[16a] and 0.8 kcal/mol (32%) larger than that for **aBIH**$^+$. The ϵ_{max} determination for **aBIH**$^+$ in AN was repeated three times giving similar values, and a similar difference was found for these compounds in MC. We do not believe that the smaller V_J found for **aBIH**$^+$ than for its **T**-linked analogues is caused by experimental error. As discussed in the accompanying paper,[17] smaller *V* values also occur for the related azo compounds and bis-diazeniums. Because $V \propto 1/d$ (eqs 1 and 4), a decrease in *d* from the 5.029 Å of the **H**-linking unit to the 4.860 Å of the **T**-linking unit (using the hydrazine separations for the neutral *t*-Bu,*i*-Pr bis-hydrazines from Table 1 as *d*) would only increase *V* from 2.50 to 2.59 (4%), so most of the increase observed presumably has another origin. *V* should be affected by lone pair, σ_{CC} overlap, and from the X-ray structures of the neutral materials, the extra twist in the center of the molecule for **aBIT**$^+$ would tend to make this overlap slightly better,[16b] although these effects appear to us too small to rationalize the observed increase in *V* in going from **H**- to **T**-linked compounds (although the X-rays are of neutral compounds, not the cations). Another factor could be that closure of the 4-membered ring in **aBIH**$^+$ creates other (longer and less well aligned) through-bond pathways, and calculations have indicated that having other pathways can decrease *V* as well as increase it.[18] We have noted that AM1 calculations provide the correct magnitude for V_{AM1} = half the AM1-UHF enthalpy difference between the ground state and excited state for cations constrained to C_2 symmetry to mimic the ET transition state, at 5.2 kcal/mol for **aBIT**$^+$ and 5.3 kcal/mol for **aBIH**$^+$,[7] but they do not predict the smaller *V* for the **H**-linked system than that of the **T**-linked system that is observed.[19] In summary, we believe that experimental data demonstrates that **H**-linked radical cations have a detectably smaller *V* than the **T**-linked ones despite the presence of very similar double four σ-bond pathways linking the dinitrogen units, but we cannot point to any single structural factor that clearly causes this to happen.

Turning to the separation of λ into λ_v and λ_s, there are obviously problems with the values derived from best fit to the CT absorption curves in various solvents (Table 3). We chose to analyze these data at $h\nu_v = 2.29$ kcal/mol (800 cm^{-1}); raising $h\nu_v$ raises the λ_s needed for fit (see Table 5). Even if the DMF data are disregarded (the values are especially strange in DMF, possibly because of the specific solvent interaction indicated below, although the difference for **aBIT**$^+$ and **sBIT**$^+$ suggests that this cannot be the only problem), obtained a 3.5 kcal/mol larger λ_s in 1,2-dichloro-ethane than in than in MC for **sBIT**$^+$ when the λ values only differ by 0.4 kcal/mol indicates to us that there must be ≥ 2 kcal/mol error in making such a separation by fitting the CT bands for these compounds. **aBIT**$^+$ in AN, BN, and MC gives an average λ_v of 30.5 kcal/mol (range +0.6, −1.0) and **sBIT**$^+$ in four solvents gives average λ_v of 30.6 (+1.7, −2.4). Only two solvents were studied for **aBIH**$^+$, and they average to an anomalously high λ_v of 38.2(±3). The λ_s obtained in MC was anomalously small, and its ($\lambda - E_{op}$) value was 4.0 kcal/mol, significantly larger than the 2.6 average (range +0.5, −0.3) for the other 10 spectra analyzed in Table 3. In retrospect, there is likely to be something wrong with the MC optical data for **aBIH**$^+$, but we report these data because there was no indication of problems while obtaining it. Despite limited data, it is clear that the solvent effects on λ are rather different for **BI**$^+$ derivatives than that for **22H**$^+$, despite having the same linking groups with four α-branched alkyl substituents for both types of compounds. Significantly poorer agreement with the dielectric continuum approximation prediction that λ will be linear with γ occurs for **BI**-substituted cations than for **22H**$^+$. Both **aBIT**$^+$ and **sBIT**$^+$ have larger λ in DMF than in AN, the opposite of the prediction from γ values. Another difference is that λ(AN) -λ(MC) is 4.5−4.2 kcal/mol for the three *t*-Bu,*i*-Pr compounds, about 1.6 times that for **22H**$^+$, which if the dielectric continuum theory of eq 6 were used would imply that λ_s(AN) were over 50% larger for the **BI**$^+$ compounds than for **22H**$^+$, which appears unreasonable because of their similar sizes. Our data suggest to us that specific solvent interaction which stabilizes the cationic center of the **BI**$^+$ compounds in AN relative to MC more than that arising from the polarity difference estimated by the dielectric continuum theory equation is occurring and that the effect is even larger for DMF, a much

(16) (a) The anamalously small value observed for **aBIT**$^+$ in DMF occurs because of a low ϵ_{max} value, which probably indicates incomplete oxidation, producing a lower concentration of cation than we assumed. (b) For **aBIT**, the Newman projection approximation (lone pairs bisecting NNR angle in a Newman projection down the NC_b bond) produces lpN,C_bC twist angles of 179.7° and 179.4° at the *inner* N-*i*-Pr nitrogens and 57.8° and 54.6° at the *outer* N-*t*-Bu nitrogens. For the less-twisted **aBIH**, these numbers are 177.0° and 177.0° (*inner* N-*i*-Pr) and 62.7° and 62.9° (*outer* N-*t*-Bu).

(17) Nelsen, S. F.; Trieber, D. A., II; Wolff, J. J.; Powell, D. R.; Rogers-Crowley, S. *J. Am. Chem. Soc.* **1997**, *119*, 6873.

(18) (a) Shepard, M. J.; Paddon-Row, M. N.; Jordan, K. D. *J. Am. Chem. Soc.* **1994**, *116*, 5328. (b) Jordan, K. D.; Paddon-Row, M. N. *Chem. Rev.* **1992**, *92*, 395.

(19) A referee pointed out that one cannot meaningfully speak of a molecule following a classical path through a particular value of a nonclassical normal coordinate, and as we pointed out,[7] the C_2-constrained structures employed are not transition states on the ground state energy surface, although they do obey the criterion that the geometries at the ends are the same, so the electron could relax to either hydrazine unit. These AM1-UHF calculations obtain $V_{AM1} = 6.1$ kcal/mol for *out*,*out* **22H**$^+$,[7] but only 3.2 for the *in*,*in* isomer. This is disturbing because everyone agrees that electronic interaction is larger for 180° twist angles than for ones near 0°,[4,19] and it is obvious that AM1 calculations may not be reliable for estimates of *V*.

better donor than a nitrile. Specific solvent stabilization of the cations by DMF is also suggested by the difference in the first two oxidation potentials being 1.1 kcal/mol smaller (23%) in DMF than in AN for **aBIT**$^+$ (Table 2). It appears, then, that having the *trans* hydrazine units lacking a second bicyclic bridge in the **BI**$^+$ compounds, which directs one isopropyl methyl group away from the NN unit, allows enough additional accessibility of solvent that specific solvation interactions become detectable; they were not observed for the perbicyclic bridged *cis* hydrazine unit **22H**$^+$.

Table 7. Predicted Effect of Temperature on k_{350}/k_{250} Values

cmpd	solvent	ESR[a]	optical[b]
22H$^+$	AN	2.1	53
aBIT$^+$	MC	8.1	76
sBIT$^+$	MC	9.6	71
aBIH$^+$	MC	14.4	[23]

[a] Calculated from the activation parameters shown in Table 4. [b] Calculated from the λ_s, λ_v, V, and $h\nu_v$ values shown in Tables 3 and 6.

Discussion. 4. Calculation of ET Rate Constants

A rate constant calculation using the Hush theory ET parameters from Tables 5 and 6, $\lambda_s = 9.0$ and $\lambda_v = 37.6$ (Figure 4), $V_H = 3.77$ kcal/mol, and $h\nu_v = 700$ cm^{-1} (2.00 kcal/mol) will be considered first. The large V_H makes the reaction adiabatic, $\kappa_{el} = 1.000$ (using eq 36 in ref 6a), and using the tunnelling factor, Γ_n, formulation (eq 64 in ref 6a), the adiabatic rate constant k_{ad} (eq 5 in ref 6a) may be written as eq 7. Using

$$k_{ad} = \nu_n \Gamma_n \exp(-\Delta G^*/k_B T) \quad (7)$$

Sutin's first-order adiabatic energy surface formulation (eq 33 in ref 6a), $\Delta G^{\ddagger}$ is given by eq 8, which makes ΔG^* 8.18 kcal/mol, which is 3.47 kcal/mol (30%) smaller than $\lambda/4$. Hush uses

$$\Delta G^* = \lambda/4 - V + V^2/\lambda \quad (8)$$

the Γ_n formulation shown in eq 9 (see eq 10 in ref 4), where $F = h\nu_v/4k_bT$. Hush's Γ_n is larger than that which Sutin employs

$$\Gamma_n = [2F\ \mathrm{csch}(2F)]^{-1/2} \exp\{[-\lambda_v/h\nu_v][\tanh(F) - F]\} \quad (9)$$

(eq 69 in ref 6a) by the factor containing csch(2F), which is 1.24 for our data, and although both are only supposed to apply when $h\nu_v$ is less than $2k_BT$, and $h\nu_v$ is $1.7(2k_BT)$ for the present case, we use eq 9 anyway, since we lack an alternative. The k_{ad} at 25 °C obtained is 4.9×10^8 s^{-1}, 3.7 times larger than the experimental value.

The ET rate constant using vibronic coupling theory is given by eq 10.[11−13] It is important to replace the eq 2 FC(g) with

$$k_{et} = [4\pi^2/h]V^2 \mathrm{FC}_{v,w}(g) \quad (10)$$

$\mathrm{FC}_{v,w}(g)$ (see eq 11),[12] which includes sums in both the starting material and product wells to properly evaluate k_{et} at $g = 0$, as is necessary for the $\Delta G = 0$ thermal ET reactions under consideration. Using Jortner theory, the ET rate constant is the

$$\mathrm{FC}_{v,w}(g) = (4\pi\lambda_s k_B T)^{-1/2} \times [\textstyle\sum_v \exp(-vh\nu_v/RT)]^{-1} \sum_v \sum_w F(v,w) \exp(-vh\nu_v/RT) \times \exp[-(\lambda_s + \{w - v\}h\nu_v + g)^2/4\lambda_s RT] \quad (11A)$$

$$F(v,w) = \exp(-S) v!w![\textstyle\sum_r \{(-1)^{v+w-r} S^{(v+w-r)/2}\}/ \{r!(v-r)!(w-r)!\}]^2 \quad (11B)$$

sum of individual ($v \rightarrow w$) and ($w \rightarrow v$) rate constants whose weighting is determined by eq 11, and increasingly large error is introduced by using only the single sum FC(g) expression of eq 2 in eq 10 as $h\nu_v$ decreases below about 1200 cm^{-1}.[20] The proper vibronic coupling theory k_{cal}(298 K) value using eq 10 and the ET parameters for **22H**$^+$ from the Jortner theory analysis with $h\nu_v = 750$ cm^{-1} (those shown in Table 6) is 6.5×10^6 s^{-1}. This makes k_{ESR}/k_{cal} (AN, 298 K) = 20. Because the Jorner analysis lowers V and raises λ relative to the Hush analysis, agreement with experiment is better when Hush-theory-derived ET parameters are employed in eq 10 (as we did previously),[5,7] but we do not think that this can be justified now that a Jortner theory analysis of the parameters is available.

The calculated ET rate constants for the *t*-Bu,*i*-Pr compounds at 298 K using the Jortner analyses of the CT bands in the solvents for which ESR data are available are included in Tables 3 and 6 and are compared with the ESR rate constants in Table 4. Agreement is not very good, k_{ESR}/k_{cal} values ranging from 20 to 36 (ignoring the **aBIH**$^+$ number, which rather clearly has something wrong with it from internal comparisons). With so many parameters, we could obviously make agreement look better by adjusting some of them in the "right" directions, and plausible arguments could be made for such adjustments. Nevertheless, such parameters would not fit the CT bands as well as the ones given.

Although agreement of k_{ESR} with k_{cal} is slightly better for **22H**$^+$ than it is for the *t*-Bu,*i*-Pr compounds, this is only because comparison was made at 298 K, where the optical spectra were measured. As pointed out before, the small temperature sensitivity observed for k_{ESR} for **22**$^+$ is very different from that calculated using eq 10 and could only be rationalized if tunneling were for some reason much more important than predicted.[7] Table 7 shows a comparison of the k_{350}/k_{250} ratios expected from the ESR activation parameters with the those expected using the optical data from Tables 3 and 6. Although we realize that the optical parameters are likely to change some with temperature, we are not even sure of the sign of the change in λ_s[21] and just use constant ET parameters here.

Disscussion. 5. Conformational Differences between 22H$^+$ and *t*-Bu,*i*-Pr Compounds

The major structural difference between the perbicyclic **22H**$^+$ and their *t*-Bu,*i*-Pr analogues, which have unlinked *N*-alkyl substituents, is that the former has *cis* hydrazine units and the latter *trans* ones, as indicated in the drawings of the "mono-

(20) Figure 8 of ref 7, which plots V vs $h\nu_v$ for **22H**$^+$ data using both the single- and double-sum FC equations, has a serious error at small $h\nu_v$ values for the double sum (introduced by a programming error). The proper double-sum V, $h\nu_v$ pairs are 6.57 kcal/mol at 800 cm^{-1} and 4.63 kcal/mol at 900 cm^{-1}. This changes a statement in ref 7: the Jortner V, $h\nu_v$ curve does *not* bend over to approach Sutin's "first order adiabatic" rate V (ref 6a, p 455) as $h\nu_v$ approaches zero, but continues to rise.

(21) From data given by Grampp (Grampp, G.; Jaenicke, W. *Ber. Bunsen-Ges. Phys. Chem.* **1991**, *95*, 904), $\gamma_{350}/\gamma_{250} = 0.98$ for CH_2Cl_2, but is 1.06 for CH_3CN, therefore λ_s should change slightly in opposite directions for these two solvents using dielectric continuum theory (which does not work properly for our compounds). We have not investigated temperature effects on the optical spectra of these compounds, but for a related alkyl,aryl bis-hydrazine, λ_s increases as the temperature is lowered in CH_2Cl_2, but V calculated using eq 3 increases more than enough to compensate for this. We shall discuss temperature effects on the optical spectra of organic intervalence compounds separately.

mers", **22/22** and **22/BI**. We suggest that these conformational differences may be responsible for some of the differences in their spectral and ET behavior.

V_J in AN for **22H**$^+$ at 3.22 kcal/mol is 0.7 kcal/mol (24%), larger than that for **aBIH**$^+$ at 2.5 kcal/mol. Although the extra two bicyclic rings of **22H**$^+$ may induce more twist at the nitrogen bonds for this compound, we suggest that their difference in conformation is likely to be more important. **aBIH**$^+$ has *trans* hydrazine units, so the two $N^+-C_b-C-C_b-N$ four σ-bond shortest pathways between the oxidized and reduced hydrazine units will be different, and only one can have the higher *V* lone pair *out* overlap situation (marked "higher" on the **aBIH**$^+$ structure below). Neutral **22H** is shown by ^{13}C

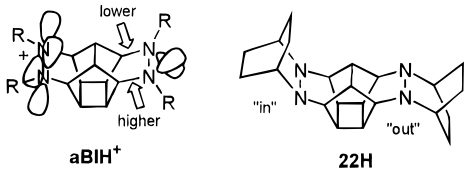

aBIH$^+$ **22H**

NMR to exist principally in the *in*,*out* conformation.[7] The nitrogens at the oxidized hydrazine unit are flattened substantially, interconversion between the two double nitrogen inversion forms is very rapid, and the spectra that we observe are presumably the superposition of spectra for both forms, although we do not know their energy difference. If the neutral hydrazine unit of **22H**$^+$ remains *in*, both lone pairs would be in the more favorable σ_{CC} *out* configuration, and perhaps that is why we see a larger *V* for **22H**$^+$ than for **aBIH**$^+$ despite their having the same linking unit.

k_{ESR} is significantly more sensitive to temperature for all three *t*-Bu,*i*-Pr compounds studied than it is for **22H**$^+$ (Table 7). We believe that this is likely to be associated with conformational effects of the *cis* hydrazine units of **22H**$^+$. We do not know the ratio of *in* to *out* bicyclic substituents in **22H**$^+$, but ET should be significantly faster when both the oxidized and reduced forms are in the same double-nitrogen inversion form, because ET is thermoneutral then, but is endothermic if the hydrazine unit configurations do not match. If the equilibrium constant for *in*/*out* at the oxidized hydrazine were not close to 1.0 and the major isomer did not match that of the reduced side, the conformational change at the oxidized hydrazine unit would appear as a fast equilibrium before the ET step, and the $\Delta H°$ and $\Delta S°$ would be incorporated into the observed activation parameters. We expect that such a prior equilibrium should not be occurring for the **BI**$^+$ isomers, because the nitrogen substituent disposition is imposed by the linking group, which seems consistent with the larger and closer to theoretical expectation temperature sensitivity of k_{ESR} for these compounds.

Discussion. 6. Possible Causes for the Discrepency between k_{cal} and k_{ESR}

Although the temperature sensitivity observed for k_{ESR} of the *t*-Bu,*i*-Pr substituted compounds is closer to that predicted than for **22H**$^+$, it is still not large enough, and their k_{cal}(298 K) values are too small. An obvious possibility for problems is inappropriate partitioning of λ. Internal vibrations which are small enough (below ca. k_BT) should actually be part of λ_s and not λ_v (despite their designations).[22] This might be especially significant for hydrazines: the dynamics analysis by AM1 for **22H**$^+$ gave the result that 36% of the internal vibrational energy was accounted for by modes with $h\nu_v$ of 71 and 143 cm^{-1},[7] which are below *kT* and presumably actually a part of λ_s for the purposes of Jortner theory. Although we appreciate that the AM1 frequencies are likely to be calculated poorly and, indeed, that low-frequency vibrations are probably overemphasized by this method,[7] we think it is worth examining what happens if the 71 and 143 cm^{-1} modes are assigned as part of λ_s instead of λ_v. This raises the $\langle h\nu_v \rangle$ prediction to 1028 cm^{-1}, and the observed CT band is then best fit using $\lambda = 49.5$ (essentially unchanged), $V = 3.23$ (essentially unchanged), with $\lambda_s = 28.5$ kcal/mol and $\lambda_v = 21.0$ kcal/mol. This transfer of low-frequency modes from λ_v to λ_s significantly lowers *S* (to 7.1) and results in an eq 10 prediction of $k_{298} = 4.4 \times 10^6$ s^{-1}, slightly *poorer* agreement with experiment than not doing the transfer. We believe that this shows that the separation of λ_v and λ_s is not the principal problem in acheiving agreement between theory and experiment for bis-hydrazine radical cations.

A second possibility is that we have just used the single frequency approximation for the vibronic coupling theory, and a single frequency approximation may just not be sufficient for compounds with as large λ_v as these. The small change in predicted rate constant when large variations of λ_v and λ_s were tried above makes us suspect that this is not the real problem.

Another possibility is that the CT band analysis centers on the $0,w \approx S$ transitions, and *S* is 17.6 for **22H**$^+$ and 13.6 for **aBIT**$^+$ in AN using the data from Tables 6 and 3. The thermal rate constant experimentally measured, however, is determined by much smaller v,w transitions. The increments to the observed rate constant are dominated by $v,w \leq 2$, and very small when $v,w > 4$. Any deviations from harmonicity going to rather high vibrational excitations would affect the prediction, and we do not know how large these effects might be. We return to this question in related work, where bis-diazenium radical cations are studied.[17]

Conclusions

Using Jortner theory instead of Hush theory to extract the ET parameters from CT absorption bands raises the estimated λ and lowers the estimated *V*, both of which make agreement with experimental rate constants poorer when Jortner theory is used to estimate the ET rate constant. Separation of λ_v from λ_s in fitting the CT bands considered here is inaccurate, both because of strong interaction between $h\nu_v$ and the λ_v,λ_s partitioning and the fact that small differences in the shape of the wings strongly affect the partitioning obtained. Transferring the expected relatively large contribution of low-frequency λ_v modes to λ_s, as expected to occur using Jortner theory, makes agreement of k_{cal} with experiment worse. The anomalously small ESR k_{350}/k_{250} ratio observed for the *cis*-fused perbicyclic system **22H**$^+$ becomes larger for the *trans*-fused *t*-Bu,*i*-Pr compounds, suggesting to us that hydrazine conformation might be involved in causing this result, but even the latter compounds exhibit smaller ratios than predicted. Harmonicity of the nested parabolas (Figure 3) would have to be maintained to *w* values above 14 for Jortner-theory-derived ET parameters to fit thermal ET rate constants quantitatively, which might cause problems. Although **22H**$^+$ CT bands follow the expectation of dielectric continuum theory that λ is proportional to γ, the donating solvent DMF causes higher λ for both diastereomers of **BIT**$^+$, suggesting that specific solvent interaction with the oxidized hydrazine unit is occurring, even for these quite hindered compounds.

Experimental Section

General. Instrumentation is the same as described elsewhere,[17] except that a Brucker AM 500 spectrometer was used for some NMR spectra. Subscripted numbers in NMR data strings indicate standard deviation.

(22) For example, see: ref 12 (paragraph 3, section 5). (a) Zeng, Y.; Zimmt, M. B. *J. Phys. Chem.* **1992**, *96*, 8395. (b) Barbara, P. F.; Meyer, T. J.; Ratner, M. A. *J. Phys. Chem.* **1996**, *100*, 13148 (see p 13157).

2,7-Di-*tert*-butyl-3,8-diisopropyl-2,3,7,8-tetraazahexacyclo-[7.4.1.0^{4,12}.0^{5,14}.0^{6,11}.0^{10,13}]tetradecane (aBIH) was prepared and purified by the same method used for **s**- and **aBIT**,[9] starting with the *anti*-bis-diazenium salt **aBH**$^{2+}$(BF$_4^-$)$_2$[2] (77.0 mg, 0.162 mmol), giving **aBIH** as a white solid (61 mg, 97%): mp 157−158 °C; ^{1}H NMR (CD_2Cl_2) δ 3.22 (septet, J = 7.0 Hz, 1H), 3.12 (septet, J = 7.0, 1H), 3.01 (bs, 2H), 2.92 (bs, 1H), 2.62 (complex, 6H), 1.25 (d, J = 6.6 Hz, 3H), 1.15 (s, 9H), 1.06$_9$ (d, J = 7.0 Hz, 3H), 1.06$_5$ (s, 9H), 1.06$_3$ (d, J = 6.6 Hz, 3H), 1.01 (d, J = 7.0 Hz, 3H); ^{13}C NMR (CD_2Cl_2) δ 58.93, 58.78, 56.93, 566.68, 52.91, 52.43, 51.76, 51.42, 38.89, 38.41, 37.88, 36.3, 34.52, 34.08, 29.23, 29.05, 20.61, 20.48, 19.21, 18.86; MS calcd for $C_{24}H_{42}N_4$ 386.3413, found 386.3049. Crystals of **aBIH** for the X-ray crystal structure determination were grown from ethanol. The structure was determined at 133(2) K using a 0.42 × 0.25 × 0.20 mm crystal, on a Siemens P4/CCD diffractometer using Mo Kγ radiation (λ = 0.710 73 Å), Wyckoff scan type, θ range from 3.0 to 25.0°. The solution of the structure with direct methods used Siemens software, which refines on F^2 values.[23] X-ray data: $C_{22}H_{42}N_4$, fw 386.62, monoclinic, space group $P2_1/n$, unit cell dimensions a = 8.2788(2), b = 23.3285(2), and c = 12.1110(2) Å, β = 106.162(2)°, V = 2246.58-(7) Å^3, Z = 4, D_{calcd} = 1.143 mg/m^3, absorption coefficient = 0.068 mm^{-1}, F(000) = 856; reflections collected = 8664, independent reflections = 4518 [R_{int} = 0.0217], data = 4518, restraints = 12 (disorder), parameters = 279, goodness-of-fit (on F^2) = 1.202, final R indices [$I > 2\sigma(I)$] R_1/wR2 = 0.0640/0.1280, R indices (all data) R_1/wR2 = 0.0753/0.1331, extinction coefficient = 0.0036(7), largest difference peak/hole = 0.311/−0.203 e Å^{-3}, largest and mean Δ/esd 0.0080/0.004.[24] The *t*-Bu and *i*-Pr groups were slightly disordered; the major conformation present is the *t*-Bu *in* (toward the central CC bond of the molecule), *i*-Pr *out* (that shown in the drawing of **aBIH** in the Introduction), but ~8% of the *t*-Bu *out*, *i*-Pr *in* conformation (double nitrogen inverted at both hydrazine units) was also present in the crystal, modeled as C(15) and C(24) [*t*-Bu methyl groups in the major conformation] with occupancies of 0.918(4), and C(17a) and C(26a) [methyl groups not present in the major conformation] with occupancies of 0.082(4). Only the major conformation is considered in Table 1.

Oxidation to Radical Cations. *Electrochemical* oxidations used the apparatus described elsewhere.[17] For coulometric oxidation, 20 mL of 0.1 M tetrabutylammonium perchlorate solution was preelectrolyzed for 1 h at a potential 0.5 V positive of $E_1°$ of the compound to be studied and 12 mL were removed and stored in a volumetric flask under nitrogen. Solid bis-hydrazine, typical sample size 2 mg, was added to the well, dissolved (heating is required for CH_3CN as solvent), dearated with nitrogen, and electrolyzed at 0.3 V positive of $E_1°$. Typical oxidations took from 15 to 30 min. The electrolyzed solution was removed with a gas-tight syringe, transferred to a volumetric flask, and diluted to the mark with the preelectrolyzed solvent.

Silver nitrate oxidations were carried out in deaerated solvents and typically employed 2 mg samples of bis-hydrazine, and 1 equiv of $AgNO_3$ at known concentration was added by syringe (typically < 30 μL), resulting in an instant color change and formation of gray precipitate. After stirring 8 min of stirring, the solution was filtered through a 1 in. plug of Celite into a volumetric flask, and the reaction flask and Celite were washed with solvent as the sample was diluted to the mark. The time from the beginning of the oxidation to data acquisition was usually under 20 min.

Dynamic ESR simulations employed program ESREXN by J. Heinzer, QCPE program 209, with modifications by Peter A. Petillo and Rustem F. Ismagilov to run on IBM-PC clones and a Unix computer (IBM RS-6000). The rate constants determined at each temperature are summarized in Table 8, and the activation parameters from these rate constants appear in Table 4.

Table 8. Rate Constants Obtained by Dynamic ESR Simulations in Methylene Chloride

cmpd	T (K)	k_{ESR} (10^7 s^{-1})
aBIT$^{+\,a}$	303.8	11.2
	294.3	10.3
	283.9	8.0
	274.7	6.3
	264.3	4.8
sBIT$^{+\,a}$	303.9	10.5
	294.0	9.1
	284.0	7.0
	274.2	5.3
	264.4	4.2
aBIH$^{+\,b}$	308.1	15.5
	303.2	14.5
	293.3	11.0
	283.2	8.2

[a] Simulation parameters: a(2N) = 13.3 G, a(2H) = 2.6 G, a(4H) = 0.6 G, line width = 1.1 G. [b] Simulation parameters: a(2N) = 13.3 G, a(4H) = 0.6 G, line width = 1.1 G. Fits are noticably poorer for **aBIH**$^+$; the experimental specta appear as if they have better resolution of the lines than the calculated ones.[10]

Acknowledgment. We thank the National Science Foundation for partial financial support of this research under Grant CHE 9417946 and the National Science Foundation, the National Institutes of Health, and the University of Wisconsin for funds used in purchacing the spectrometers and computers used in this work. We thank NATO for a travel grant which allowed the participation of J.J.W. in the synthetic work. We are especially indebted to Ralph Young (Kodak) and Marshall Newton for helpful discussions and to an exceptionally helpful referee.

JA963415M

(23) Data collection: SMART Software Reference Manual (1994). Data reduction: SAINT version 4 Software Reference Manual (1995). Solution, refinement, and graphics: G. M. Sheldreick (1994), SHELXTL version 5 Reference Manual, all from Siemens Analytical X-ray Instruments, 6300 Enterprise Dr., Madison, WI 53719-1173. Neutral atom scattering factors were taken from *International Tables for Crystallography*; Kluwer: Boston, 1992; Vol. C, Tables 6.1.1.4, 4.2.6.8, and 4.2.4.2.

(24) The authors have deposited atomic coordinates for this structure with the Cambridge Crystallographic Data Centre. The coordinates can be obtained, on request, from the Director, Cambridge Crystallographic Data Centre, 12 Union Road, Cambridge, CB2 1EZ, U.K.